

Measurements of Cabibbo Suppressed Hadronic Decay Fractions of Charmed D^0 and D^+ Mesons

M. Ablikim¹, J. Z. Bai¹, Y. Ban¹¹, J. G. Bian¹, X. Cai¹, J. F. Chang¹,
 H. F. Chen¹⁶, H. S. Chen¹, H. X. Chen¹, J. C. Chen¹, Jin Chen¹, Jun Chen⁷,
 M. L. Chen¹, Y. B. Chen¹, S. P. Chi², Y. P. Chu¹, X. Z. Cui¹, H. L. Dai¹,
 Y. S. Dai¹⁸, Z. Y. Deng¹, L. Y. Dong^{1a}, Q. F. Dong¹⁵, S. X. Du¹, Z. Z. Du¹,
 J. Fang¹, S. S. Fang², C. D. Fu¹, H. Y. Fu¹, C. S. Gao¹, Y. N. Gao¹⁵, M. Y. Gong¹,
 W. X. Gong¹, S. D. Gu¹, Y. N. Guo¹, Y. Q. Guo¹, K. L. He¹, M. He¹², X. He¹,
 Y. K. Heng¹, H. M. Hu¹, T. Hu¹, X. P. Huang¹, X. T. Huang¹², X. B. Ji¹,
 C. H. Jiang¹, X. S. Jiang¹, D. P. Jin¹, S. Jin¹, Y. Jin¹, Yi Jin¹, Y. F. Lai¹, F. Li¹,
 G. Li², H. H. Li¹, J. Li¹, J. C. Li¹, Q. J. Li¹, R. Y. Li¹, S. M. Li¹, W. D. Li¹,
 W. G. Li¹, X. L. Li⁸, X. Q. Li¹⁰, Y. L. Li⁴, Y. F. Liang¹⁴, H. B. Liao⁶, C. X. Liu¹,
 F. Liu⁶, Fang Liu¹⁶, H. H. Liu¹, H. M. Liu¹, J. Liu¹¹, J. B. Liu¹, J. P. Liu¹⁷,
 R. G. Liu¹, Z. A. Liu¹, Z. X. Liu¹, F. Lu¹, G. R. Lu⁵, H. J. Lu¹⁶, J. G. Lu¹,
 C. L. Luo⁹, L. X. Luo⁴, X. L. Luo¹, F. C. Ma⁸, H. L. Ma¹, J. M. Ma¹, L. L. Ma¹,
 Q. M. Ma¹, X. B. Ma⁵, X. Y. Ma¹, Z. P. Mao¹, X. H. Mo¹, J. Nie¹, Z. D. Nie¹,
 H. P. Peng¹⁶, N. D. Qi¹, C. D. Qian¹³, H. Qin⁹, J. F. Qiu¹, Z. Y. Ren¹, G. Rong¹,
 L. Y. Shan¹, L. Shang¹, D. L. Shen¹, X. Y. Shen¹, H. Y. Sheng¹, F. Shi¹,
 X. Shi^{11c}, H. S. Sun¹, J. F. Sun¹, S. S. Sun¹, Y. Z. Sun¹, Z. J. Sun¹, X. Tang¹,
 N. Tao¹⁶, Y. R. Tian¹⁵, G. L. Tong¹, D. Y. Wang¹, J. Z. Wang¹, K. Wang¹⁶,
 L. Wang¹, L. S. Wang¹, M. Wang¹, P. Wang¹, P. L. Wang¹, S. Z. Wang¹,
 W. F. Wang^{1d}, Y. F. Wang¹, Z. Wang¹, Z. Y. Wang¹, Zhe Wang¹, Zheng Wang²,
 C. L. Wei¹, D. H. Wei¹, N. Wu¹, Y. M. Wu¹, X. M. Xia¹, X. X. Xie¹, B. Xin^{8b},
 G. F. Xu¹, H. Xu¹, S. T. Xue¹, M. L. Yan¹⁶, F. Yang¹⁰, H. X. Yang¹, J. Yang¹⁶,
 Y. X. Yang³, M. Ye¹, M. H. Ye², Y. X. Ye¹⁶, L. H. Yi⁷, Z. Y. Yi¹, C. S. Yu¹,
 G. W. Yu¹, C. Z. Yuan¹, J. M. Yuan¹, Y. Yuan¹, S. L. Zang¹, Y. Zeng⁷, Yu Zeng¹,
 B. X. Zhang¹, B. Y. Zhang¹, C. C. Zhang¹, D. H. Zhang¹, H. Y. Zhang¹,
 J. Zhang¹, J. W. Zhang¹, J. Y. Zhang¹, Q. J. Zhang¹, S. Q. Zhang¹,
 X. M. Zhang¹, X. Y. Zhang¹², Y. Y. Zhang¹, Yiyun Zhang¹⁴, Z. P. Zhang¹⁶,
 Z. Q. Zhang⁵, D. X. Zhao¹, J. B. Zhao¹, J. W. Zhao¹, M. G. Zhao¹⁰, P. P. Zhao¹,
 W. R. Zhao¹, X. J. Zhao¹, Y. B. Zhao¹, H. Q. Zheng¹¹, J. P. Zheng¹, L. S. Zheng¹,
 Z. P. Zheng¹, X. C. Zhong¹, B. Q. Zhou¹, G. M. Zhou¹, L. Zhou¹, N. F. Zhou¹,
 K. J. Zhu¹, Q. M. Zhu¹, Y. C. Zhu¹, Y. S. Zhu¹, Yingchun Zhu^{1e}, Z. A. Zhu¹,
 B. A. Zhuang¹, X. A. Zhuang¹, B. S. Zou¹.

(BES Collaboration)

¹ Institute of High Energy Physics, Beijing 100049, People's Republic of China

² China Center for Advanced Science and Technology (CCAST), Beijing 100080,
 People's Republic of China

³ Guangxi Normal University, Guilin 541004, People's Republic of China

⁴ Guangxi University, Nanning 530004, People's Republic of China

⁵ Henan Normal University, Xinxiang 453002, People's Republic of China

⁶ Huazhong Normal University, Wuhan 430079, People's Republic of China

⁷ Hunan University, Changsha 410082, People's Republic of China

- ⁸ Liaoning University, Shenyang 110036, People's Republic of China
⁹ Nanjing Normal University, Nanjing 210097, People's Republic of China
¹⁰ Nankai University, Tianjin 300071, People's Republic of China
¹¹ Peking University, Beijing 100871, People's Republic of China
¹² Shandong University, Jinan 250100, People's Republic of China
¹³ Shanghai Jiaotong University, Shanghai 200030, People's Republic of China
¹⁴ Sichuan University, Chengdu 610064, People's Republic of China
¹⁵ Tsinghua University, Beijing 100084, People's Republic of China
¹⁶ University of Science and Technology of China, Hefei 230026, People's Republic of China
¹⁷ Wuhan University, Wuhan 430072, People's Republic of China
¹⁸ Zhejiang University, Hangzhou 310028, People's Republic of China
- ^a Current address: Iowa State University, Ames, IA 50011-3160, USA.
^b Current address: Purdue University, West Lafayette, IN 47907, USA.
^c Current address: Cornell University, Ithaca, NY 14853, USA.
^d Current address: Laboratoire de l'Accélérateur Linéaire, F-91898 Orsay, France.
^e Current address: DESY, D-22607, Hamburg, Germany.

Abstract

Using data collected with the BESII detector at e^+e^- storage ring Beijing Electron Positron Collider, the measurements of relative branching fractions for seven Cabibbo suppressed hadronic weak decays $D^0 \rightarrow K^- K^+$, $\pi^+ \pi^-$, $K^- K^+ \pi^+ \pi^-$ and $\pi^+ \pi^+ \pi^- \pi^-$, $D^+ \rightarrow \bar{K}^0 K^+$, $K^- K^+ \pi^+$ and $\pi^- \pi^+ \pi^+$ are presented.

PACS: 13.25.Ft, 14.40.Lb

1 INTRODUCTION

Hadronic decays of charmed mesons have been extensively studied. Measurements of relative lifetimes and semileptonic branching fractions for charmed mesons D^+ and D^0 suggest the presence of nonleptonic processes which enhance the D^0 and suppress the D^+ width, and lead to the conclusion that the simple spectator model of charmed-meson decay is inadequate. As shown in Figure 1, all weak decays of heavy mesons may be described by six quark-diagrams: the external W-emission diagrams (a), the internal W-emission diagrams (b), the W-exchange diagram (c), the W-annihilation diagram (d), the horizontal W-loop diagram (e), and the vertical W-loop diagram (f) [1]. Thus, a further understanding of the D decay mechanism, such as the contributions of other quark-diagrams and final states interactions, requires a systematic study of the hadronic decays.

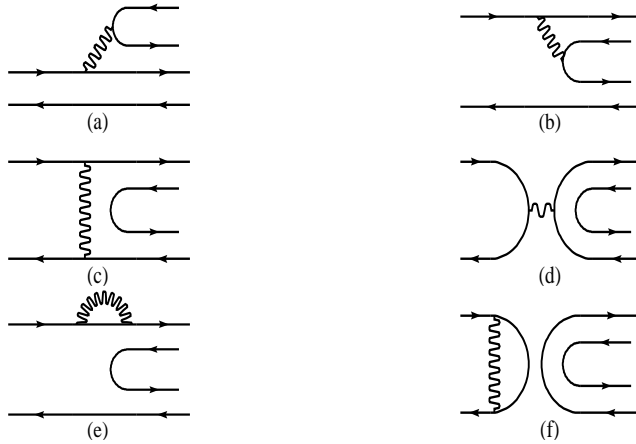


Fig. 1. Typical Feynman diagrams for Cabibbo suppressed decays of charm mesons.

At present, many experiments, such as, MARKII [2], MARKIII [3], E691 [5], E687 [6], E791 [4], FOCUS [8] and CLEO [7], have reported their measurements of Cabibbo suppressed hadronic decay fractions of D mesons. Our present measurements are based on a data sample of integrated luminosity of $\sim 17.3\text{pb}^{-1}$ at $\psi(3770)$ peak ($\sqrt{s} = 3.773$ GeV) and $\sim 16.5\text{pb}^{-1}$ for $\psi(3770)$ peak scan collected by Beijing Spectrometer (BESII) detector at e^+e^- storage ring Beijing Electron Positron Collider (BEPC) [9]. This paper reports our measurements of Cabibbo suppressed relative branching fractions for several hadronic decay modes of charmed D mesons $D^0 \rightarrow K^-K^+$, $\pi^+\pi^-$, $K^-K^+\pi^+\pi^-$, $\pi^+\pi^+\pi^-\pi^-$, $D^+ \rightarrow \bar{K}^0K^+$, $K^-K^+\pi^+$ and $\pi^-\pi^+\pi^+$ (through out this paper the charge conjugate states are implicitly included).

2 BESII DETECTOR

The Beijing Spectrometer (BESII) is a conventional cylindrical magnetic detector that is described in detail in Ref. [10]. A 12-layer Vertex Chamber (VC) surrounds the beryllium beam pipe and provides trigger information, as well as coordinate information. A forty-layer main drift chamber (MDC) located just outside the VC yields precise measurements of charged particle trajectories with a solid angle coverage over 85% of 4π ; it also provides ionization energy loss (dE/dx) measurements which are used for particle identification. Momentum resolution of $1.7\%\sqrt{1+p^2}$ (p in GeV/ c) and dE/dx resolution for hadron tracks of $\sim 8\%$ are obtained. An array of 48 scintillation counters surrounding the MDC measures the time of flight (TOF) of charged particles with a resolution of about 200 ps for hadrons. Outside the TOF counters, a 12 radiation length, lead-gas barrel shower counter (BSC), operating in limited streamer mode, measures the energies of electrons and photons over 80% of the total solid angle with an energy resolution of $\sigma_E/E = 0.22/\sqrt{E}$ (E

in GeV). Outside the solenoidal coil, which provides a 0.4 T magnetic field over the tracking volume, is an iron flux return that is instrumented with three double-layer muon counters that identify muons with momentum greater than 500 MeV/ c .

In this analysis, a GEANT3 based Monte Carlo package (SIMBES [11]) with detailed consideration of the detector performance (such as dead electronic channels) is used. The consistency between data and Monte Carlo has been carefully checked in many high purity physics channels, and the agreement is reasonable.

3 EVENT SELECTION

Charged tracks are required to satisfy $|\cos \theta| < 0.8$, where θ is the polar angle in the MDC, and have good helix fit. The tracks that are not associated with K_S^0 reconstruction are required to be originate from interaction point. Pions and kaons are identified by requiring the confidence level of desired hypothesis using combined measurements of time-of-flight [14] and energy loss in drift chamber to be greater than 0.1%. In addition, kaon and pion candidates are further identified by requiring the normalized weights, which is defined as $CL_\alpha / (CL_\pi + CL_K)$, where α denotes desired particle, exceeding 50%.

K_S^0 candidates are detected through the decay of $K_S^0 \rightarrow \pi^+ \pi^-$. Each oppositely charged track pair is assumed to be π^+ and π^- . The decay vertex of K_S^0 is required to be 5mm far away from the beam axis. The $\pi^+ \pi^-$ invariant mass is required to be within 0.020 GeV/ c^2 of the K_S^0 nominal mass.

Cabibbo suppressed hadronic decay modes are expected at a lower rate ($\sim \tan^2 \theta_C$, where θ_C is ‘‘Cabibbo angle’’) compared to relevant Cabibbo favoured modes, for which π/K misidentification becomes significant. The unique energy of D meson at the $\psi(3770)$ can be exploited to reduce explicitly background due to incorrect particle assignment. A single particle misidentification results in a reflection peak separated from the beam energy.

The distributions of energy difference (ΔE) between measured energy of D candidates (E_{tag}) and beam energy (E_b) are shown in Figure 2 for 4 Cabibbo allowed decay modes with correct π/K assignments and the reflection ΔE distribution with a single particle misidentification. ΔE of D candidate is required to be less than that of similar topological decay mode to reject particle misidentification combination. ΔE is further required to be within 50-100 MeV for different decay channels.

The pair production of $D\bar{D}$ at $\psi(3770)$ provides a variable, which is defined

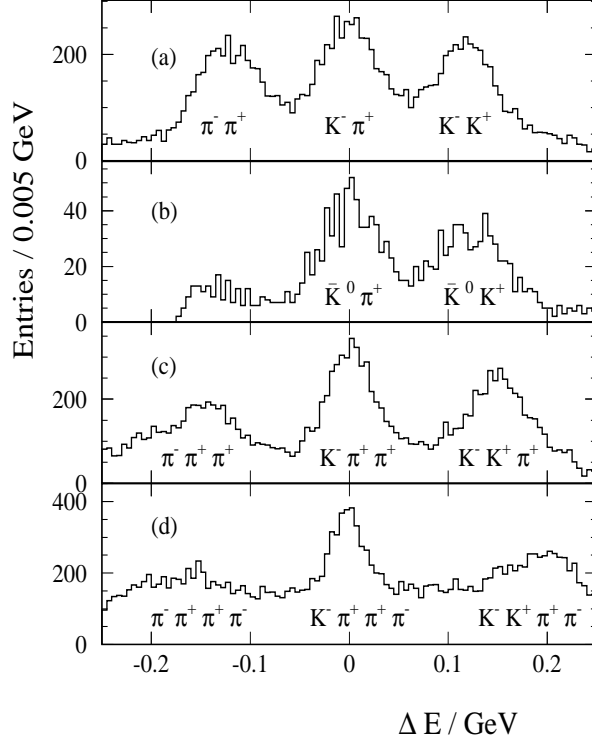


Fig. 2. ΔE distribution and reflection for similar Cabibbo suppressed modes by using the sample of Cabibbo favoured mode (a) $D^0 \rightarrow K^-\pi^+$ (b) $D^0 \rightarrow \bar{K}^0\pi^+$ (c) $D^+ \rightarrow K^-\pi^+\pi^+$ (d) $D^0 \rightarrow K^-\pi^+\pi^+\pi^-$. The distributions show the well-separated ΔE peaks.

as the beam-constrained mass

$$M_{bc} = \sqrt{E_{\text{beam}}^2 - \left(\sum_i p_i\right)^2}$$

exploiting the fact that the total energy of all decay products must sum to the beam energy. As the uncertainty in the beam energy is much smaller than the uncertainty in the total reconstructed energy of the decay tracks, this approach yields much improved mass resolution compared to the invariant mass technique.

The QED processes, $\tau^+\tau^-$ pair productions and cosmic backgrounds may contribute to D tags. Both of them have a lower multiplicity than that of $D\bar{D}$ decay, the requirement of $N_{\text{ch}} + N_{\text{neu}}/2 > 3$ will eliminate most of these backgrounds, where N_{ch} and N_{neu} represent the total number of charged tracks and neutral tracks respectively. At $\psi(3770)$, $D\bar{D}$ are produced with the angular distribution $\sin^2\theta_D$, where θ_D is the production angle of $\psi(3770) \rightarrow D\bar{D}$, $|\cos\theta_D| < 0.8$ is imposed to each D tag to enhance signal to background ratio.

One event could be counted more than once as a tag candidate. In order to calculate the actual number of tagged events in an unbiased manner, the

following criterion is applied to select only one tag combination per event: if more than one combination of tracks form the desired tag, the combination is chosen when the lowest momentum track of this combination has the largest momentum of all other combinations. The result mass plots are shown in Figure 3, 4.

4 DETECTOR ACCEPTANCE

The detection efficiency is determined by a detailed Monte Carlo simulation of $D\bar{D}$ production, decay and detector response. The decay branching ratios of neutral and charged D meson are taken from the world average values [13], some unseen decay modes are set according to the rules of isospin conservation. Simulated events are processed through the event reconstruction, selection and analysis program.

There are several sub-resonant decay modes in 3-body and 4-body Cabibbo suppressed channels. The detection efficiency is not uniform among these decay modes. The relative decay branching fractions and their errors in PDG are quoted. For $D^+ \rightarrow \pi^- \pi^+ \pi^+$ channel, $\rho^0 \pi^+$ and $\pi^- \pi^+ \pi^+$ modes are considered; for $D^+ \rightarrow K^- K^+ \pi^+$ channel, $\phi \pi^+$, $\bar{K}^{*0} K^+$ and $K^- K^+ \pi^+$ are considered; for $D^0 \rightarrow K^- K^+ \pi^+ \pi^-$ channel, $\phi \pi^+ \pi^-$, $\phi \rho^0$, $\bar{K}^{*0} K^{*0}$, $K^- K^+ \rho^0$ and $K^- K^+ \pi^+ \pi^-$ are considered; for $D^0 \rightarrow \pi^- \pi^+ \pi^+ \pi^-$ channel, the uncertainty to Monte Carlo efficiency is estimated to be less than 2%.

5 RESULTS

The observed number of each Cabibbo suppressed decay channel is determined by fitting the distributions to a function of the form:

$$F(m) = a_1 \left[m \sqrt{1 - \left(\frac{m}{E_b}\right)^2} \exp \left(a_2 \left[1 - \left(\frac{m}{E_b}\right)^2 \right] \right) \right] + a_3 \exp \left(-\frac{(m-M_D)^2}{2\sigma^2} \right) + a_4 \quad (1)$$

where the first term parameterizes the background; the Gaussian term accounts for the signal. Just above the D mass, there is no more phase space available for a decay to a pair of $D\bar{D}$ mesons. The background term is ARGUS form [12], where a_1 is the normalization factor; a_2 , a scale factor for the exponential term; E_b , the beam energy and fixed at 1.8865 GeV while fitting the mass plot. For $\psi(3770)$ scan data, the beam energy is not a constant, but the background shape is similar, a constant background term a_4 is applied to

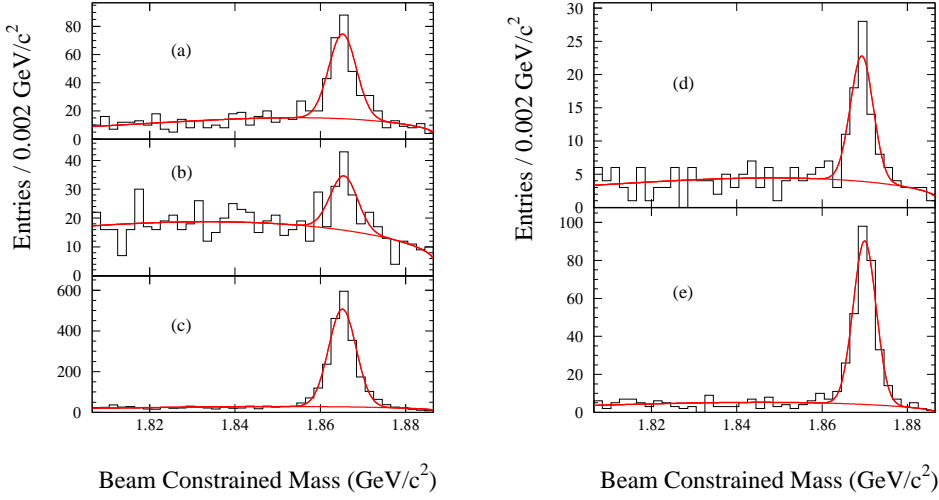


Fig. 3. Beam energy constrain mass distributions for decays (a) $D^0 \rightarrow K^- K^+$, (b) $D^0 \rightarrow \pi^- \pi^+$, (c) $D^0 \rightarrow K^- \pi^+$ and (d) $D^+ \rightarrow \overline{K}^0 K^+$, (e) $D^+ \rightarrow \overline{K}^0 \pi^+$.

evaluate the varying beam energy points. The mass resolution of each Cabibbo suppressed mode is determined by fitting the M_{bc} plot of similar Cabibbo allowed modes. The event number for each mode is summarized in Table 1.

The pions that are part of reconstructed K_S^0 's, are not used in modes $\pi\pi$, $\pi\pi\pi$, $\pi\pi\pi\pi$ and $KK\pi$, $KK\pi\pi$. However, there remain some D decays into $K_S^0\pi^+$, $K_S^0\pi^+\pi^-$ and $K^-K^+K_S^0$, where the K_S^0 is not identified as a separated vertex, which will be the major background source for decay mode $D^+ \rightarrow \pi^- \pi^+ \pi^+$ and $D^0 \rightarrow \pi^- \pi^+ \pi^+ \pi^-$, $K^- K^+ \pi^+ \pi^-$. To reduce the feed-down $K_S^0 \rightarrow \pi^+ \pi^-$ background, a cut of $|M_{\pi^+\pi^-} - M_{K^0}| > 0.040 \text{ GeV}/c^2$ is imposed on the invariant mass of each pion pairs for $\pi^- \pi^+ \pi^+$ and $K^- K^+ \pi^+ \pi^-$ modes.

For the decay $D^0 \rightarrow \pi^- \pi^+ \pi^+ \pi^-$, plots of the invariant mass of all $\pi^+ \pi^-$ combinations in D^0 candidates within the signal and sideband regions are shown in Figure 5(a) and (b) respectively. There is a clear K_S^0 peak within D^0 signal region with a fitted events number of 112.5 ± 19.0 events and no clear K_S^0 peak within the sideband region. The K_S^0 number is consistent with the expected background (Monte Carlo study gives this number as 98.8) due to $D^0 \rightarrow \overline{K}^0 \pi^+ \pi^-$. These are thus subtracted from the 4π signal.

6 SYSTEMATIC UNCERTAINTIES

In this analysis, we normalize the relative ratios of Cabibbo suppressed decay to similar Cabibbo favoured modes, which permits the cancellation of many common systematic errors. The systematic uncertainties on energy cut and

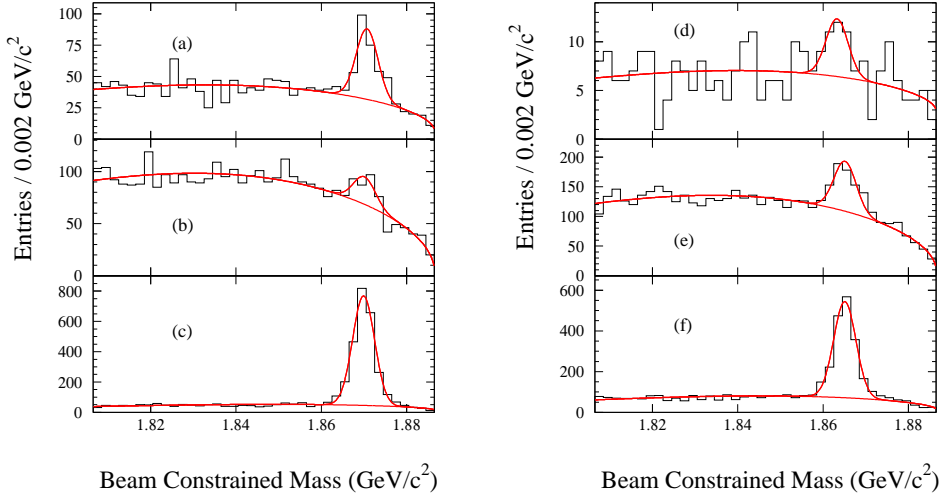


Fig. 4. Beam energy constrain mass distribution for decay (a) $D^+ \rightarrow K^- K^+ \pi^+$, (b) $D^+ \rightarrow \pi^- \pi^+ \pi^+$, (c) $D^+ \rightarrow K^- \pi^+ \pi^+$ and (d) $D^0 \rightarrow K^- K^+ \pi^+ \pi^-$, (e) $D^0 \rightarrow \pi^- \pi^+ \pi^+ \pi^-$, (f) $D^0 \rightarrow K^- \pi^+ \pi^+ \pi^-$.

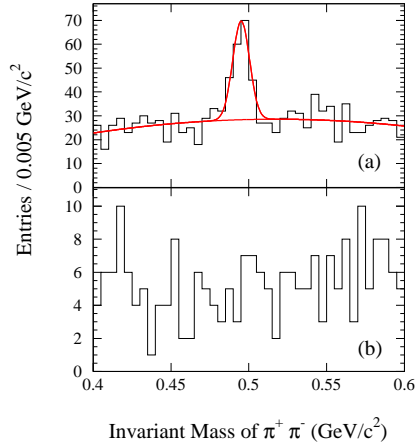


Fig. 5. $M_{\pi^+\pi^-}$ for $\pi^- \pi^+ \pi^+ \pi^-$ candidates within D^0 signal region (a) and sideband region (b).

particle identification can not be canceled completely.

Systematic uncertainties on particle identification and ΔE cuts are about 1-3 % and 1-6% contributing to the relative fractions respectively. The systematic uncertainties on background subtraction due to the K_S^0 contamination are estimated to be $\sim 2\%$ [15].

The detection efficiencies are not uniform among the different sub-resonant decay modes in the 3 and 4 body decays, 0.5 – 2.0% are estimated for different modes $\pi^- \pi^+ \pi^+$, $K^- K^+ \pi^+$ and $\pi^- \pi^+ \pi^+ \pi^-$. Large uncertainty in $K^- K^+ \pi^+ \pi^-$

mode is found due to the decays of low momentum kaons.

7 CONCLUSIONS

Table 1
Measurement results of 7 Cabibbo suppressed decay modes.

Decay mode	Yield	Relative efficiency	Branching ratio
$\frac{K^- K^+}{K^- \pi^+}$	$\frac{242.2 \pm 20.1}{1934 \pm 49}$	1.029 ± 0.017	$0.122 \pm 0.011 \pm 0.004$
$\frac{\pi^- \pi^+}{K^- \pi^+}$	$\frac{75.9 \pm 14.7}{1934 \pm 49}$	1.146 ± 0.030	$0.034 \pm 0.007 \pm 0.001$
$\frac{\overline{K^0} K^+}{K^0 \pi^+}$	$\frac{63.2 \pm 9.8}{287 \pm 18}$	0.991 ± 0.041	$0.222 \pm 0.037 \pm 0.013$
$\frac{K^- K^+ \pi^+ \pi^-}{K^- \pi^+ \pi^+}$	$\frac{181.2 \pm 20.2}{2324 \pm 53}$	$0.669 \pm 0.015 \pm 0.010$	$0.117 \pm 0.013 \pm 0.007$
$\frac{\pi^- \pi^+ \pi^+ \pi^-}{K^- \pi^+ \pi^+}$	$\frac{84.9 \pm 22.4}{2324 \pm 53}$	$0.888 \pm 0.029 \pm 0.004$	$0.041 \pm 0.011 \pm 0.003$
$\frac{K^- K^+ \pi^+ \pi^-}{K^- \pi^+ \pi^+ \pi^-}$	$\frac{19.3 \pm 8.0}{1540 \pm 51}$	$0.286 \pm 0.021 \pm 0.017$	$0.044 \pm 0.018 \pm 0.005$
$\frac{\pi^- \pi^+ \pi^+ \pi^-}{K^- \pi^+ \pi^+ \pi^-}$	$\frac{(274.4 \pm 31.8) - (112.5 \pm 19.0)}{1540 \pm 51}$	$1.336 \pm 0.028 \pm 0.027$	$0.079 \pm 0.018 \pm 0.005$

The relative fractions of seven Cabibbo suppressed decay modes are tabulated in Table.1. For each mode, fitted event number, background number, relative efficiency and relative branching ratio are listed. The errors of relative efficiency are Monte Carlo statistical error and systematic error due to sub-resonant modes respectively. The first error of branching ratio is statistical, the second one is systematic. The estimated systematic uncertainty is 3-6% for all modes, and the statistical uncertainties of the measurements are about 10% or greater. Results from this measurement are consistent with the world average values and we have improved the previous measurements of the $D^+ \rightarrow \overline{K^0} K^+$ relative branching ratio. The measurements of Cabibbo suppressed branching ratios presented here provide new insights into the mechanism of nonleptonic D decays. Exact SU(3) symmetry predicts the equality of $\Gamma(D^0 \rightarrow \pi^- \pi^+)$ and $\Gamma(D^0 \rightarrow K^- K^+)$. But the above results show they are not equal. Several distinct effects could contribute to this inequality. Final states interactions breaking SU(3) symmetry could however account for the difference.

8 ACKNOWLEDGMENTS

The BES collaboration thanks the staff of BEPC for their hard efforts. This work is supported in part by the National Natural Science Foundation of China under contracts Nos. 19991480, 10225524, 10225525, the Chinese Academy of Sciences under contract No. KJ 95T-03, the 100 Talents Program of CAS under Contract Nos. U-11, U-24, U-25, and the Knowledge Innovation Project of CAS under Contract Nos. U-602, U-34 (IHEP); and by the National Natural Science Foundation of China under Contract No. 10175060 (USTC), and No. 10225522 (Tsinghua University).

References

- [1] L.L. Chau and H.Y. Cheng, Phys. Rev. **D36**, 137(1987)
- [2] G.S. Abrams, et al., Phys. Rev. Lett. **43**, 481(1979)
- [3] R.M. Baltrusaitis, et al., Phys. Rev. Lett. **55**, 150(1985)
- [4] E.M. Aitala, et al., FNAL E791 Collab. Phys. Lett. **B421**, 405(1998); E.M. Aitala, et al., FNAL E791 Collab. Phys. Lett. **B423**, 185(1998); E.M. Aitala, et al., FNAL E791 Collab. Phys. Rev. Lett. **86**, 770(2001)
- [5] J.C. Anjos, et al., (FNAL E691 Collab.) Phys. Rev. Lett. **62**, 125(1989); J.C. Anjos, et al., (FNAL E691 Collab.) Phys. Rev. **D41**, 2705(1990); J.C. Anjos, et al., (FNAL E691 Collab.) Phys. Rev. **D43**, 635(1991); J.C. Anjos, et al., (FNAL E691 Collab.) Phys. Rev. **D44**, 3371(1991)
- [6] P.L. Frabetti, et al., (FNAL E687 Collab.) Phys. Lett. **B281**, 167(1992); P.L. Frabetti, et al., (FNAL E687 Collab.) Phys. Lett. **B321**, 295(1994); P.L. Frabetti, et al., (FNAL E687 Collab.) Phys. Lett. **B354**, 486(1995); P.L. Frabetti, et al., (FNAL E687 Collab.) Phys. Lett. **B346**, 199(1995); P.L. Frabetti, et al., (FNAL E687 Collab.) Phys. Lett. **B351**, 591(1995); P.L. Frabetti, et al., (FNAL E687 Collab.) Phys. Lett. **B407**, 79(1997)
- [7] R. Ammar et al., (CLEO Collab.) Phys. Rev. **D44**, 3383(1991); M. Bishai et al., (CLEO Collab.) Phys. Rev. Lett. **78**, 3261(1997); S.E. Csorna et al., (CLEO Collab.) Phys. Rev. **D65**, 092001(2002)
- [8] J.M. Link et al., (FNAL FOCUS Collab.) Phys. Rev. Lett. **88** 041602(2002); J.M. Link et al., (FNAL FOCUS Collab.) Phys. Lett. **B555**, 167(2003); J.M. Link et al., (FNAL FOCUS Collab.) hep-ex/0411031
- [9] C. Zhang, et al., in: J. Rossback(Ed.). HEACC'92 Hamburg, XVth Int. Conf. on High Energy Accelerators, Hamburg, Germany, July 20-24, 1992, P.409.
- [10] J.Z. Bai *et al.*, (BES Collab.) Nucl. Instr. and Meth. **A458** (2001) 627.

- [11] J. C. Chen *et al.*, BES internal report.
- [12] H. Albrecht *et al.*, Phys. Lett. **B241** (1990) 278.
- [13] Particle Data Group, Phys. Lett. **B592** (2004)
- [14] S.S. Sun, K.L. He et al., Systematic Study of Time of Flight Correction of BESII
(Submitted to HEP &NP).
- [15] Z. Wang et al., HEP &NP, 27, 1(2003).